A Study of the Effects on Langmuir Probes by Photo Electrons

by Steffen Brask, Gullik Vetvik Killie, Christian Pedersen, Yukari Sasaki, Satoki Oki, Nizam Ahmad

Abstract

Spacecraft in LEO (Low Earth Orbit) interact with the surrounding plasma in various ways. In this study we investigate if the photoelectrons emmited from the spacecraft can cause any measurable effect on Langmuir probes situated outside the spacecraft. This is done by numerical simulations with the EMSES PIC model, with elevated photoemission. A small change in the plasma was found where the Langmuir probes are situated.

0.1 Introduction

The spacecraft in space will always be affected by its environment, resulting various impacts depending on the orbit (location), types of material as well as the environment condition that changes over time (Hastings and Garrett, 1996). The most common phenomena on the spacecraft is what so called charging. The level of charging depends on the energy of particles interacting with the spacecraft. At the lower energy, the form of interaction of charged particles with the spacecraft only affect the surface part called surface charging. However, the higher energy the worse affects might be occurred on the spacecraft and in this case the charged particles can penetrate deep inside the spacecraft component resulting in so called internal charging (Fennell et al., 2001).

Charging on the spacecraft can be simulated numerically. Numerous codes have been developed to explain the behaviour of particles around the spacecraft as well as its interaction. Nevertheless, it still remains many questions since the numerical simulation is only an approximation of the real condition. However, the numerical approach has given good solutions to various applications such as spaceflight missions. The reliability of spacecraft has been proved well before launch into space. One of these effort is simulating the environment where the satellite will be placed during its mission. Many parameters has been taking into account with respect to its effect on the spacecraft. The results of the simulation can be significant point for decision maker for the spaceflight mission. This is one of reasons why this simulation is the primary interest for this study.

In this study, we attempt to simulate a spacecraft named Norsat-1 which will be placed in Low Earth Orbit (LEO) environment around 600 km altitude and polar inclination

around 98.8°. This spacecraft is planned to launch in 2017(*NorSat-1* n.d.). Our simulation was of a smaller spacecraft with dimensions $10, 10, 10$cm. This satellite has been equipped with two probes. It is interesting since this satellite will pass over the auroral region more frequently. In this region the satellite will be exposed not only to rapid variation of the thermal component of the ionosphere (Hastings, 1995), but also to high energy particles from the solar wind.

Since we use the EMSES (Electro Magnetic Spacecraft Environment Simulator) code (Miyake et al., 2013) in the simulation, it is important to point out that only the effects of background plasma as well as the photoelectrons from the sunlight are taken into account. The simulation has been done into several cases and each case has been grouped into two, i.e. plasma flows with and without the photoemission effects on the spacecraft as well as the probes. All results will be presented in detail in the specific section in this report.

0.2 Method

0.2.1 Numerical methods

To solve the problem numerically we use the EMSES code. EMSES uses the standard PIC method for plasma simulations (Birdsall and Langdon, 2004). In the code we are able to define a spacecraft body, and the code then calculates the potential on that body using the capacitance matrix method. Although EMSES has the capability to do a full electromagnetic calculation, we have opted to use the Poisson's equation solver for electrostatic problems. In the EMSES system we can define sunlit surfaces based upon an angle, and a current density. Sunlit surfaces will then emit electrons based upon a energy distribution. For a complete description of EMSES' capabilities see (Nakashima et al., 2009). Parameters are choosen to simulate the sun at the earth, but with an enhanced flux to emphasize the effect in question.

0.2.2 Theoretical calculations

$$
\begin{aligned}
I_i &= \begin{cases} A|q|n_\infty\sqrt{\frac{8kT_i}{\pi m_i}}(without flow) \\ \frac{1}{6}A|q|n_\infty V + \frac{5}{6}A|q|n_\infty\sqrt{\frac{8kT_i}{\pi M_i}}(with flow) \end{cases} \\
I_e &= -A|q|n_\infty\sqrt{\frac{8kT_e}{\pi m_e}}exp\Big(\frac{|q|\Phi_d}{kT_e}\Big) \\
I_{ph} &= \frac{1}{6}AJ_s
\end{aligned}
\tag{0.1}
$$

Case	Plasma flow	Photon emission
1:	41600 $\vec{e_x}$ m/s	0
2:	-41600 $\vec{e_z}$ m/s	0
3:	-41600 $\vec{e_y}$ m/s	0
4:	41600 $\vec{e_x}$ m/s	$-10^{-3}A/m^3$ $\vec{e_x}$
5:	-41600 $\vec{e_z}$ m/s	$-10^{-3}A/m^3$ $\vec{e_x}$
6:	-41600 $\vec{e_y}$ m/s	$-10^{-3}A/m^3$ $\vec{e_x}$

Table 0.1: The six different cases we investigate, $1-3$ is without a photoemission, and $4-6$ is the same cases with photoemission.

Submitting these equations to $I_i + I_e + I_{ph} = 0$ and solving for Φ_d, we can get

$$\begin{aligned}
\Phi_d =& \frac{kT_e}{|q|} ln\Big(\sqrt{\frac{T_i}{T_e}}\sqrt{\frac{m_e}{m_i}} + \frac{J_s}{6n_\infty|q|}\sqrt{\frac{\pi m_e}{8kT_e}}\Big) + \Phi_0 \\
\Phi_d =& \frac{kT_e}{|q|} ln\Big(\frac{5}{6}\sqrt{\frac{T_i}{T_e}}\sqrt{\frac{m_e}{m_i}} + \frac{V}{6}\sqrt{\frac{\pi m_e}{8kT_e}} + \frac{J_s}{6n_\infty|q|}\sqrt{\frac{\pi m_e}{8kT_e}}\Big) + \Phi_0 \\
\Phi_0 =& kT_{ph},\ V = speed\ of\ flow
\end{aligned} \tag{0.2}$$

The theory is based on thin-sheath approximation, so if spacecraft size is much larger than the local Debye length, we can use it.

0.2.3 Test case setup

We wish to simulate the effects of Photon emitted electrons in different test cases, and have thus set up the following 6 cases:

Stepsize	Timestep	Density	$\|B\|$	T_e	T_i	N_x
1.0cm	5E − 10s	1.0E5kg/cm^3	50E − 6 T	3000K	1500K	128

Table 0.2: Input parameters in EMSES

So test case 1-4, 2-5, and 3-6 are the "same" cases except that we run the simulation with and without photon emission to compare the cases two and two. We define 3 geometric objects, the spacecraft itself and two probes. In all cases the B field is in the $\vec{e_z}$ direction.

0.3 Results

0.3.1 Photoelectron Trajectories

The electrons emitted from the spacecraft due to the photoelectric effect, have a kinetic energy corresponding to a Maxwellian distribution with a temperature of $T_{ph} = 3.8481 \cdot$

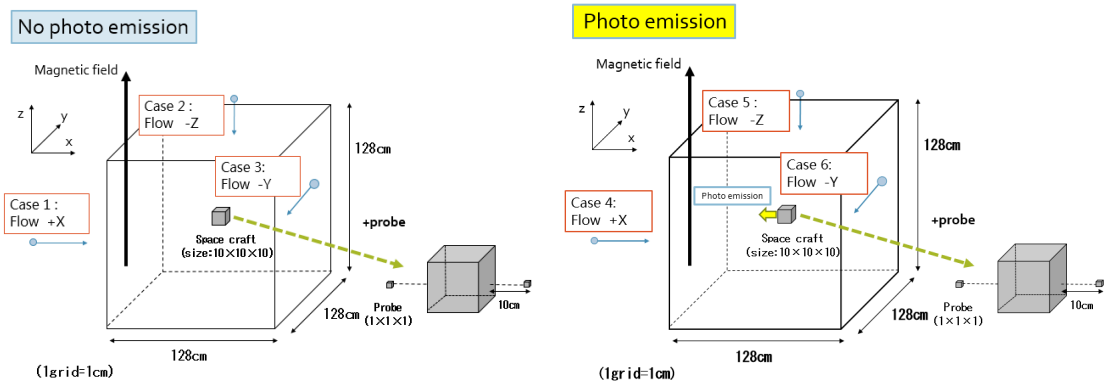

Figure 0.1: Geometry of spacecraft and surroundings without P-E and without. Left figure is no P-E simulation cases.Right figure is P-E simulation cases.

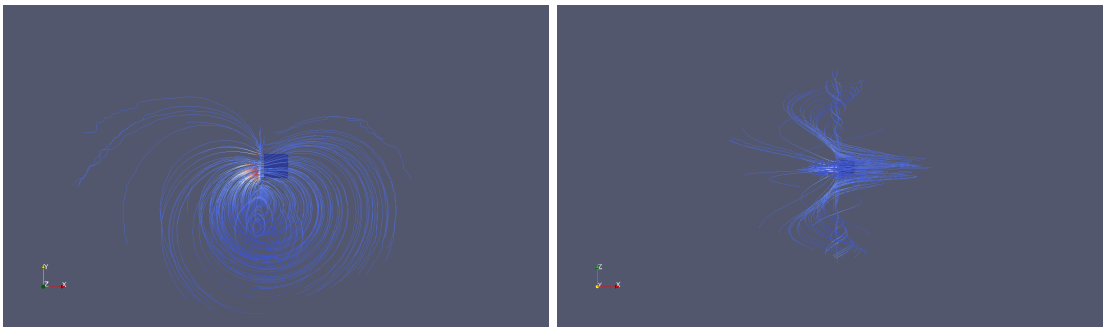

Figure 0.2: The trajectories of the electrons emitted by the photoelectric effect in simulation 6. The possible paths of the photoemitted electrons coincide with the volume occupied by the langmuir probes. The photoemitted electrons are strongly affected by the magnetic field $\vec{B}$, and follows a gyrating path guided by $\vec{B}$. The photoemitted electrons are in all the studied cases emitted from the spacecraft in $-x$ direction, and the paths are similar. The langmuir probes are situated 10cm to each side of the spacecraft along the $x-$direction.

10^4K. Figure 0.2 illustrates the trajectories of the emitted electrons in simulation 6. As the probes are situated 10cm to the sides of the spacecraft on the $x-$axis, the probes may be hit by the photo-emitted electrons. In the following section, 0.3.2, we show the number of electrons hitting the probes.

0.3.2 Accumulated Photoelectrons on Langmuir Probes

In the simulations both electrons and photoelectrons are absorbed by the probes. Table 0.3 shows the current of both regular electrons, as well as photoelectrons, interacting with the probes. The photoelectrons are emitted on the left side of the spacecraft and we see a larger current of photoelectrons here. The current caused by the photoemission is $10-100$ smaller than the current from the electrons in the plasma. This photoelectrons may

	probe to +x	probe to −x
case 1	2.207E−07	2.851E−07
case 2	2.794E−07	2.807E−07
case 3	2.786E−07	2.772E−07
case 4	2.117E−07	2.609E−07
case 5	2.754E−07	2.616E−07
case 6	2.777E−07	2.512E−07

	probe to +x	probe to −x
case 4	2.3324E−09	3.49699E−08
case 5	1.9598E−09	3.51036E−08
case 6	1.3824E−09	3.66922E−08

Figure 0.3: The left table shows the electron current (A) hitting the inserted probes at for the simulated cases $1-6$. On the table to the right the photoelectrons hitting the probes are shown. The photoelectron current is smaller than the electron current from the plasma, varying from $10-100$ times smaller.

	Without flow	With flow
Without Photon emission	-0.893	-0.792
With Photon emission	-0.718	-0.662

Table 0.3: The potential, in V, of the spacecraft computed with the thin sheet approximation, 0.2.2.

0.3.3 Spacecraft Potential

There is a difference between the theoretical and numerical potential, see section 0.3.6 for the numerical results, because λ_D is not much smaller then the length of the satellite, which is an assumption in the thin sheet approximation. From these calculations we can, however, expect the potential over the spacecraft to rise in the cases where we have photon emission.

0.3.4 Induced electric current

The plasma is flowing in in relation to the coordinate system in the simulations. Due to this an induced electrical field, ε, will appear. The induced electrical field, ε, will balance the magnetic part of the Lorentz force, $\vec{v} \times \vec{B}$. Combined with the electrostatic approximation we can obtain the ε.

$$\vec{\varepsilon} = \vec{v_D} \times \vec{B} \tag{0.3}$$

This will cause a potential gradient perpendicular to the plasma flow and the magnetic field, using the electrostatic approximation we obtain the magnitude of the gradient.

$$\int E dx = -\phi \tag{0.4}$$

$$\phi = -\int \vec{v}_d \times \vec{B} \approx -\int \left(41600\text{m/s} \cdot 50E-6\text{T}\right) dx \tag{0.5}$$

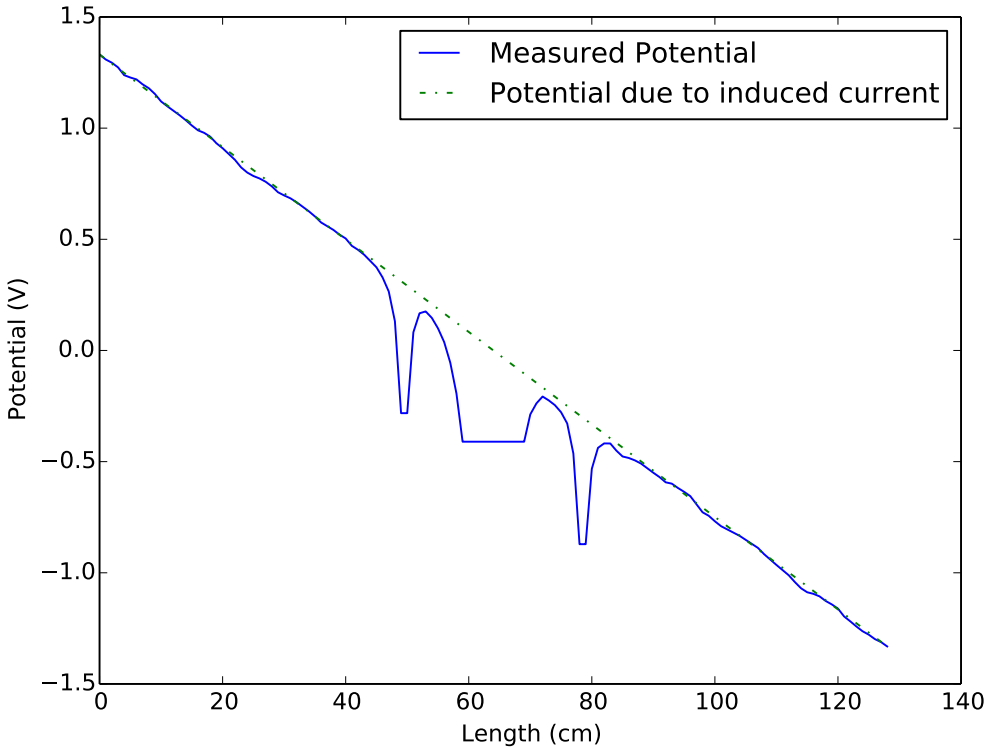

Figure 0.4: The blue line is the potential along direction x for simulation 6. In this case the potential gradient is along the $x-$axis. The dotted green line is the potential caused by the induced electrical field. This should be accounted for if we want to find the potential at the spacecraft and the probes.

$$|\nabla\phi| = 2.08\mathrm{m}^{-1} \tag{0.6}$$

Figure 0.4 shows the measured potential at case 6. In section 0.3.6, we compare the cases where the flow is in the same direction to avoid having to correct for this effect.

0.3.5 Wake plots

The spacecraft is moving relative to the plasma flow, this causes a wake to be formed in the vicinity of the craft. Figures 0.5 illustrates the flow in case $1, 2$ and 3. In case 1 the right probe is in the wake, and in both the other cases the two probes aren't affected by the wake.

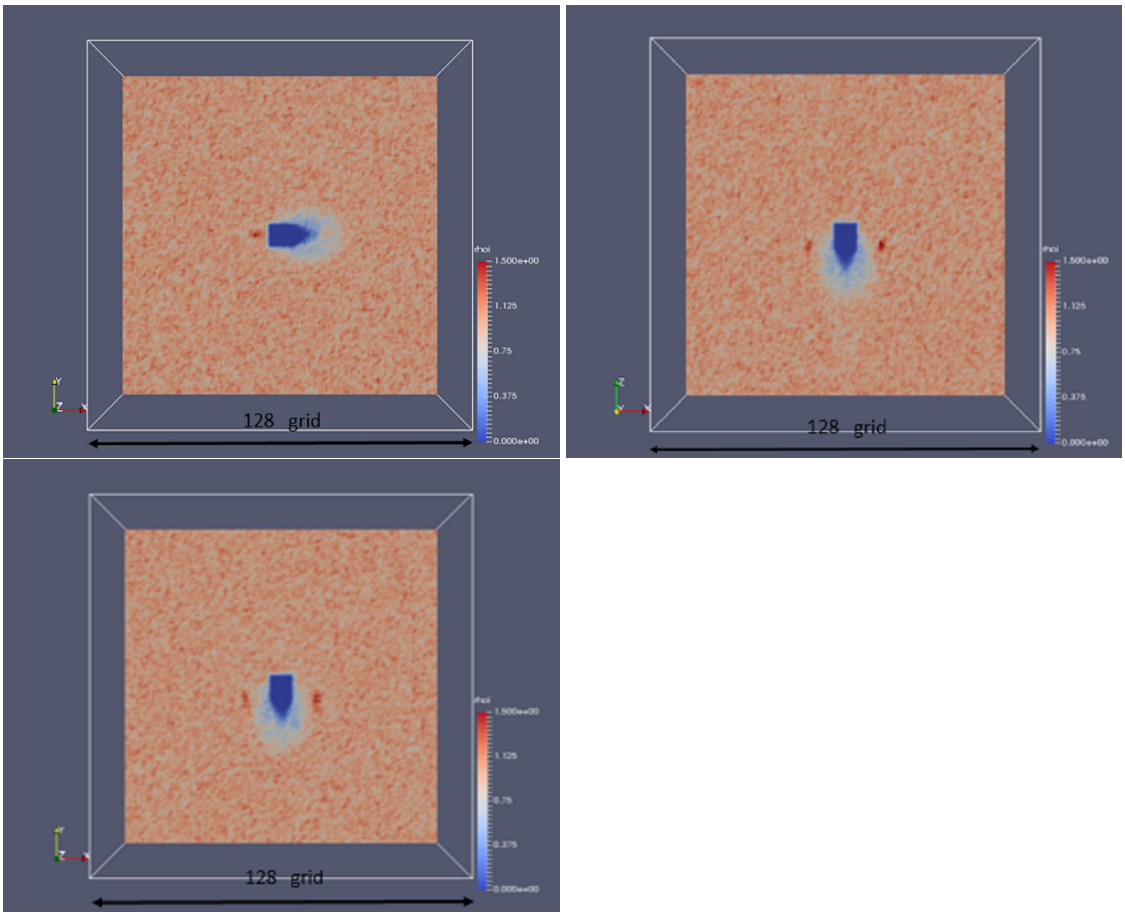

Figure 0.5: Ion density of spacecraft and surroundings without P-E. The figure on the top-left displays case 1. The top-right figure displays case 2 and the bottom-left figure displays case 3. Each grid point is 1cm.

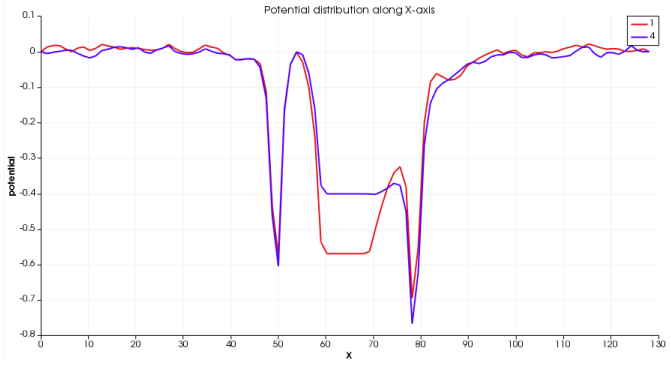

Figure 0.6: Potential [V] of satellite and surroundings in the x-direction for case 1 and case 4. Note that the potential drop is much greater in the right probe when comparing the two cases.

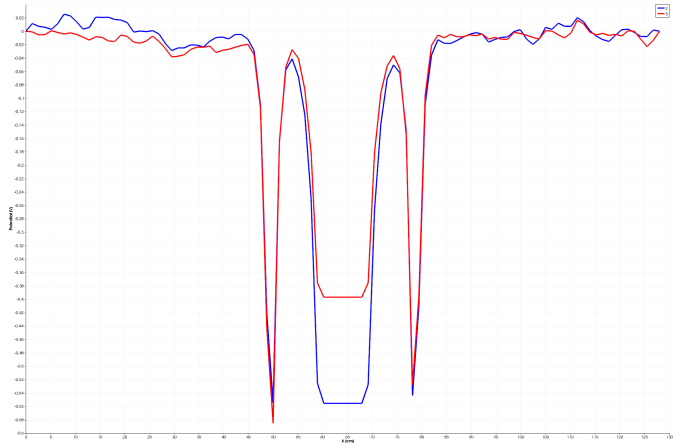

Figure 0.7: Potential of satellite and surroundings in the x-direction for case 2 and 5. Note that we have a small potential drop in the left probe but a potential rise in the right probe when comparing the two cases.

0.3.6 Potential difference with P-E and no P-E

Case 1 vs case 4

In case 4 we have the emitted electrons in the negative flow direction. As expected this leads to a drop in potential in the left probe which is facing the plasma flow as can be seen in figure 0.6. The potential drop over the probe is 0.02V or 3.8%. The right probe is now the wake where we have a drop in the ion density. This yields a large drop in potential compared to the left probe, but it also has a larger potential drop than the left probe when comparing case 1 and 4. This might be because the increase in electron density on the left side redirects more ions from the right side. The potential drop in the right probe comparing the two cases is 0.07V or 10%. The potential rise over the satellite is 0.17V or 28%.

Case 2 vs case 5

With the flow of emitted electrons in the negative x direction we would expect a rise in electron density around the left probe. This can be seen in figure 0.7 where we see a 0.03V drop in the potential of this probe compared to case 5 with no emitted electrons. On the right probe we have a small rise in the potential of 0.02V. With no emitted electrons on this side of the satellite the rise in potential can be explained by looking at the increase in ion density as seen in figure 0.5. In the satellite we have a potential rise of 0.16V which is a 28% increase. So the change in potential in the probes are small compared to the change in the satellite.

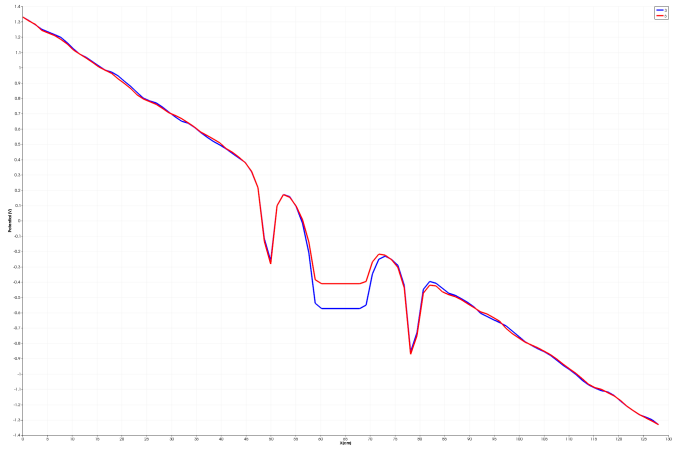

Figure 0.8: Potential of satellite and surroundings in the x-direction for case 3 and 6. Note that there is almost the same drop in potential for both probes.

Case 3 vs case 6

As we can see in figure 0.8 we have almost the same change in potential over both probes of about 0.03V. However this change yields a 12% decrease in potential for the left probe but a mere 3% increase for the right probe. Over the satellite we have a potential rise of 0.15V which yields a 26% change.

0.4 Discussion

We compared P-E and without P-E. We think whether photo emission affect the Probes. We set the size of the Probes to 1 cm^3 in this simulation. But it is the same size as the grid. So density does not become 0 in the inner of Probes. We need to simulate a variety of sizes. We try the case of more number of grid, longer a grid, and size of Probes. In order to measure the characteristic value of each particle, we set probes in the place that the wake is formed or not. But they are not a real physical model. (For example, if we give probes the photoelectric effect or if we change the size of satellite and probes to realistic scales, the results might be changed.) We see a difference in cases, so it might be a case we have not considered that that is significant.

0.5 Conclusions

We see a difference in the potential on the probes from the non photon emission cases versus the photon emission cases, and this effect is predicted. We have also shown that there is a difference in how great this change in potential is from probe right, to probe left. The magnitude of this change is dependent on the direction of the plasma flow. Although this effect is not significant in our simulations, there might be a case where it is significant if the magnetic field or the photon emission direction is changed.

In the LEO regime, where the simulations have been done, the photoemitted currents are weak compared with background plasma. Due to this the effect seen on the Langmuir probes were small, further studies should be done in other plasma regimes where the photoemmision is more pronounced, i.e. MEO, GEO or in the magnetospheric tail lobes. It should also be mentioned that a better numerical model for the Langmuir probes should be implemented in further studies.

Bibliography

Birdsall, C. and A. Langdon (2004). *Plasma Physics via Computer Simulation*. Series in Plasma Physics and Fluid Dynamics. Taylor & Francis. ISBN: 9780750310253. URL: https://books.google.co.jp/books?id=S2lqgDTm6a4C.

Fennell, J. et al. (2001). *Spacecraft charging: Observations and relationship to satellite anomalies*. Tech. rep. DTIC Document.

Hastings, D. and H. B. Garrett (1996). *Spacecraft–environment interactions*. English. Includes bibliographical references (p. 281-289) and index. Cambridge ; New York : Cambridge University Press. ISBN: 0521471281 (hc).

Hastings, D. (1995). "A review of plasma interactions with spacecraft in low Earth orbit". In: *Journal of Geophysical Research: Space Physics* 100.A8, pp. 14457–14483.

Miyake, Y. et al. (2013). "Plasma particle simulations of wake formation behind a spacecraft with thin wire booms". en. In: *Journal of Geophysical Research: Space Physics* 118.9, pp. 5681–5694. ISSN: 2169-9402. DOI: 10.1002/jgra.50543. URL: http://onlinelibrary.wiley.com/doi/10.1002/jgra.50543/abstract (visited on 27/10/2016).

Nakashima, H. et al. (2009). "OhHelp: a scalable domain-decomposing dynamic load balancing for particle-in-cell simulations". en. In: ACM Press, p. 90. ISBN: 978-1-60558-498-0. DOI: 10.1145/1542275.1542293. URL: http://portal.acm.org/citation.cfm?doid=1542275.1542293 (visited on 27/10/2016).

NorSat-1. https://directory.eoportal.org/web/eoportal/satellite-missions/n/norsat-1. Accessed: 2016-11-28.